

PAPER

MHD limit cycles on FTU

To cite this article: G. Pucella *et al* 2017 *Nucl. Fusion* **57** 116037

View the [article online](#) for updates and enhancements.

You may also like

- [Observation of the high-density edge transport barrier in CHS using beam emission spectroscopy](#)
T Oishi, S Kado, M Yoshinuma et al.
- [Effect of fatliquor level on the physical quality of Indonesian rabbit fur leather](#)
T Maryati, T Nugroho, Sundari et al.
- [Influence of plasma flow shear on tearing in DIII-D hybrids](#)
R.J. La Haye, C.C. Petty, P.A. Politzer et al.

MHD limit cycles on FTU

G. Pucella, E. Giovannozzi, P. Buratti and C. Cianfarani

ENEA, Fusion and Nuclear Safety Department, C. R. Frascati, Via E. Fermi 45, 00044 Frascati (Roma), Italy

E-mail: gianluca.pucella@enea.it

Received 18 May 2017, revised 6 July 2017

Accepted for publication 14 July 2017

Published 17 August 2017



Abstract

The development of low-order tearing modes during density ramp-up in the high density regime on the Frascati Tokamak Upgrade is characterized by an initial ordinary stage, with a ‘one-to-one’ relation between mode amplitude and frequency, followed by the formation, on the amplitude/frequency plane, of ‘limit cycles’ with increasing area up to disruption for density limit if the density continues to grow. A critical mode amplitude for transition from smooth to cyclic behavior has been observed in experiments performed changing the line-averaged density, and the existence of such a threshold has been confirmed in experiments of real time control of tearing mode in the high density regime by means of electron cyclotron resonance heating.

The amplitude and frequency modulations of the observed $m/n = 2/1$ tearing mode (m and n are the poloidal and toroidal mode number, respectively) occur in few milliseconds, which is not in agreement with the diffusion resistive time of about two hundred milliseconds expected on the $q = 2$ resonance from the non-linear theory. The origin of such modulations has been investigated, taking into account that in the high amplitude stages of the mode temporal evolution it is difficult to discriminate between non-linear effects and mode coupling mechanisms. Our analysis suggests that the formation of limit cycles could be due to a recursive island fragmentation, with a sort of self-healing phenomenon; in fact the island distortion increases before amplitude drops. Concerning the interaction with modes of different helicity, our experiments seem to indicate that the presence of the $q = 3$ resonance in the plasma is necessary for the occurrence of deep and regular limit cycles for the $2/1$ tearing mode.

Keywords: tearing mode, magnetic island, limit cycle

(Some figures may appear in colour only in the online journal)

1. Introduction

The capability to operate at high plasma densities is a crucial point in tokamak fusion devices, due to the strong dependence of the fusion reactor rate on the plasma density [1]. However, the achievable density in tokamak plasmas is observed to be limited by the appearance of events causing a rapid loss of plasma confinement, so defining an operational limit [2]. The complex phenomenology observed approaching the density limit cannot be described in detail by a simple model; nevertheless, the fact that ultimately it is a low-order tearing mode (TM) [3] which plays a crucial role is well recognized [4, 5]. The appearance of a low-order tearing mode when the density increases towards the limit is usually ascribed to the

increasing radiation loss near the edge region. The ensuing contraction of the temperature profile leads to a shrinkage of the current profile that drives unstable the tearing mode, leading to disruption if the density continues to grow, with a final stage of the mode temporal evolution characterized by a continuous increase of the mode amplitude and a continuous decrease of the mode frequency, due to a braking torque which originates from eddy currents induced by the rotating mode in the conducting shell surrounding the plasma [6].

Dedicated experiments were performed in the past on the Frascati Tokamak Upgrade (FTU) [7] to study in detail the high density regime [8]. All the investigated pulses present a very similar MHD phenomenology during the pre-programmed plasma density ramp-up, with the development

of large-amplitude TM approaching the density limit [9]. The mode temporal evolution shows a complex behavior, that can be outlined in three stages [10]. First stage: the magnetic island grows smoothly at constant rotation frequency. Second stage: amplitude and frequency feature large cycles of oscillations, with peak amplitude increasing progressively across cycles. Third stage: the island grows quickly to large amplitude and locks; this stage generally ends in a disruption. The amplitude and frequency oscillations show a well defined phase portrait, determining a so-called ‘limit cycle’ on the amplitude/frequency plane, observed for the first time on FTU. The existence of a stage with large amplitude and frequency modulations could be caused either by interaction between modes of different helicity or by island self-healing phenomena.

In this paper, we report on the observation and analysis of MHD limit cycles on FTU. The rest of the paper is organized as follows. In section 2 the experimental set-up and the data processing are described, while in section 3 the phenomenology of the observed MHD activity is illustrated. Section 4 is dedicated to the characterization of the transition between smooth and cyclic behaviors in terms of plasma parameters and mode amplitude and in section 5 the MHD limit cycles are analyzed in the phase-space ($B_{\theta 1}, \dot{B}_{\theta 1}$) to understand the origin of amplitude and frequency modulations of the observed TM. In the last section, the main results are summarized.

2. Experimental set-up

FTU is a compact device with circular poloidal cross-section ($R_0 = 0.935$ m, $a = 0.30$ m), with the capability to operate in a wide range of toroidal magnetic field ($B_T = 2 \div 8$ T) and plasma current ($I_p = 0.2 \div 1.6$ MA) values. The magnetic activity is analyzed by means of poloidal and toroidal arrays of magnetic pick-up coils installed inside the vacuum vessel at 6 different toroidal and 34 different poloidal positions inside the ports behind the toroidal limiter structure and the poloidal limiter. Regarding the signal processing, the output of the pick-up coils is processed by means of a median filter and it is integrated to obtain the poloidal magnetic perturbation associated to the MHD modes. In particular, a high-pass filter (1 kHz) is applied to eliminate slow drifting of the integral and a low-pass filter (20 kHz) is applied to eliminate noise. The Hilbert transform is used to calculate the amplitude and phase of signal starting from the poloidal magnetic perturbation and the derivative of the phase with respect to time is performed to obtain the mode frequency. Finally, a low-pass filter is used on both amplitude and frequency to decrease the associated noise. We also considered that an air core transformer was present on the MHD signal acquisition path. The resulting frequency dependent attenuation $G(f)$ (particularly strong on lower frequencies) was analytically calculated and fitted against experimental data (as derived through comparison with a transformer-free acquisition chain), with a best fit given by $G(f) = 0.568 \times f / \sqrt{f^2 + f_0^2}$, where the mode frequency f is in kHz and $f_0 = 7.1$ kHz. The resulting correction was applied to obtain the final MHD amplitudes.

It is worth noting that, different modes could be present in the same pulse. For this reason, for each frequency obtained from the magnetic pick-up coil experimental signals, a mode analysis is performed in order to identify the mode numbers m and n , by fitting phase differences between coils located at different poloidal and toroidal positions; in particular, only the main modes characteristic for FTU are searched: 2/1, 3/1, 3/2 and 4/2. If multiple modes are present at the same frequency, only the dominant one is selected by the analysis.

3. Phenomenology of the MHD activity

The time traces of some relevant quantities for the MHD activity observed in the high density regime on FTU are reported in figure 1 (left side), for a pulse with $B_T = 4.0$ T and $I_p = 0.7$ MA. The onset of a coherent activity is identified at $t = 0.82$ s, when the frequency takes a well defined value of 6.6 kHz. The analysis of the mode numbers, reported in figure 1 (right side), shows that the observed activity can be associated essentially to a $m/n = 2/1$ TM. The temporal evolution of the TM during the density ramp-up is characterized by a ‘regular stage’ (from $t = 0.82$ s to $t = 0.91$ s in the figures) where the mode amplitude increases at approximately constant frequency, and a ‘bursting stage’ (from $t = 0.91$ s to $t = 0.96$ s) where the amplitude and the frequency of the mode oscillate. Finally the mode amplitude rapidly grows up to high values and the mode frequency strongly decreases up to the disruption.

From a closer inspection of data it is possible to see that both the amplitude and frequency oscillations are higher for higher values of the line-averaged density (linearly proportional to the time for the pulse considered here). In particular, if we report the temporal evolution of the mode on the amplitude/frequency plane (see figure 2, left side), we can observe, after the regular stage (cyan lines), the formation of ‘limit cycles’ with increasing area. It is worth noting that this particular behavior has been observed for the first time on FTU [10]. In the other devices, the final stage of the mode temporal evolution is characterized by a continuous increase of the mode amplitude and a continuous decrease of the mode frequency, always keeping a one-to-one relation in the amplitude/frequency plane. As a comparison, the temporal evolution of the amplitude upper envelope and the frequency lower envelope for the pulse considered here (figure 2, right side) is also reported as open circles in figure 2 (left side).

4. Critical mode amplitude

The critical mode amplitude for transition from smooth to cyclic behavior (reported as a yellow circle in figure 2, left side) has been analyzed in a wide range of values for the toroidal magnetic field (from 4 to 8 T) and the plasma current (from 0.5 to 0.9 MA), considering ohmic pulses with increasing density up to the disruption for density limit. As we have seen, during a density ramp-up in the high density regime, the onset of a 2/1 TM occurs, followed by the appearance of limit cycles if the density continues to grow, so that it is possible to pass from the regular to the bursting stage

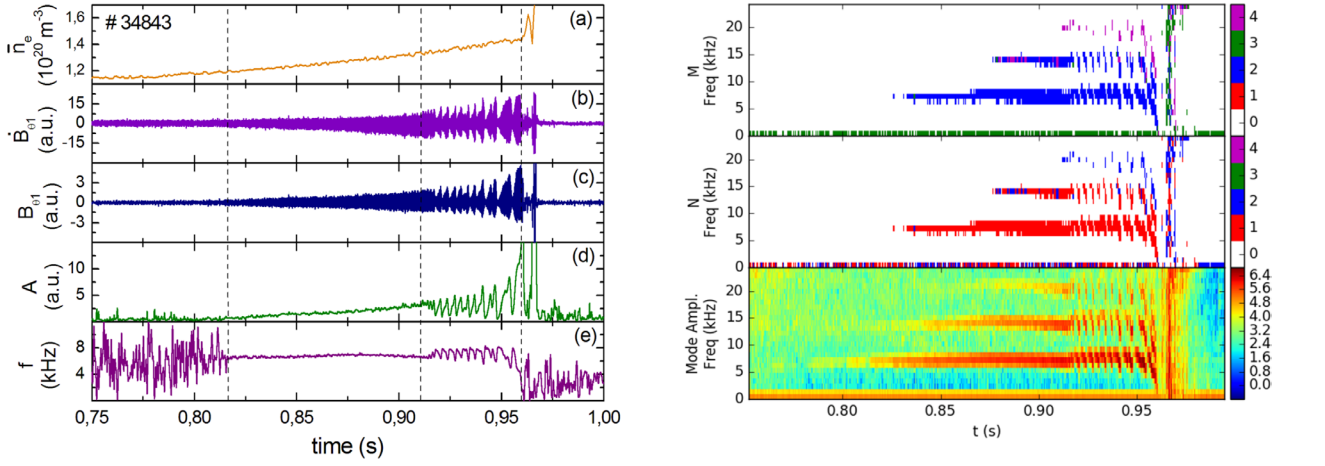


Figure 1. (Left side) Time traces of some relevant quantities for the MHD activity for a specific pulse on FTU with $B_T = 4.0$ T and $I_p = 0.7$ MA: (a) central line-averaged density, (b) output from the pick-up coil, (c) poloidal magnetic perturbation, (d) mode amplitude, (e) mode frequency. Dashed vertical lines indicate the time corresponding to the mode onset ($t = 0.82$ s) and the bursting stage (from $t = 0.91$ s to $t = 0.96$ s). Signals after $t = 0.96$ s are spurious. (Right side) From bottom to top: spectrogram of magnetic field perturbation at magnetic sensors, with colors representing the common logarithm of zero-to-peak amplitude in arbitrary units; spectrogram with colors representing toroidal and poloidal mode number for pixels with logarithm of amplitude larger than 5. The presence of overtone harmonics in the spectrogram is mainly due to the fact that signals are non sinusoidal.

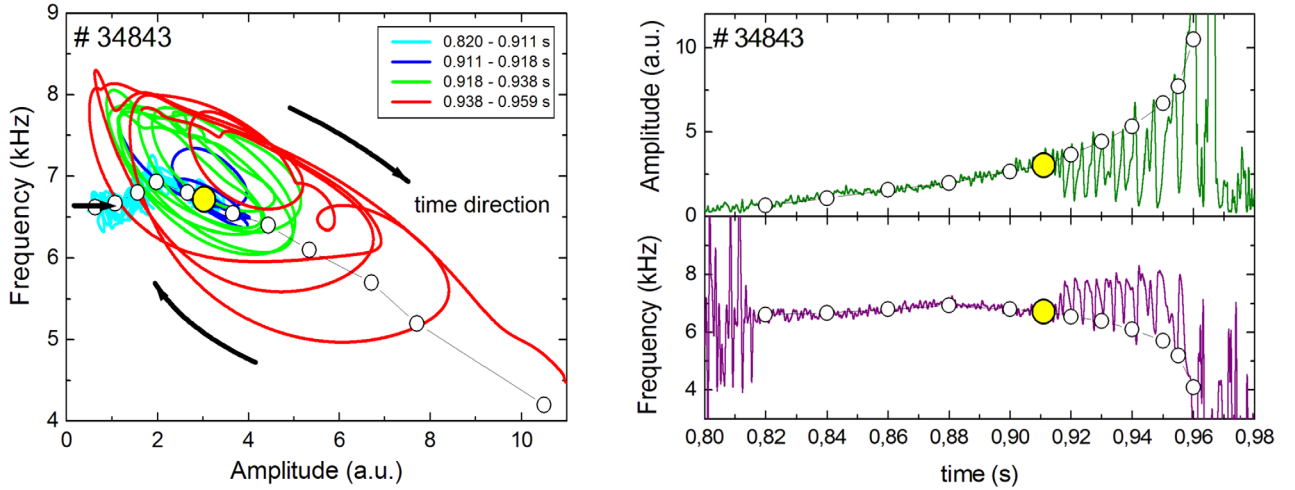


Figure 2. (Left side) Temporal evolution of the tearing mode on the amplitude/frequency plane (see the legend for the meaning of colors). The evolution of the amplitude and frequency envelopes is also reported as open circles. The yellow circle corresponds to the critical mode amplitude for transition from smooth to cyclic behavior. (Right side) Temporal evolution of the amplitude and frequency and of their envelopes.

changing the density. In other words, the idea is to obtain the dependence of the critical mode amplitude on B_T and I_p , utilizing the density as the operational parameters allowing the transition from the regular to the bursting stage for a given (B_T, I_p) configuration. A first result of this study is that the line-averaged density for the appearance of limit cycles results to be a function of the toroidal magnetic field only, with best fit values (in units of 10^{20} m^{-3}) given by $\bar{n}_{LC} = 0.19 \times B_T^{1.4}$. This result is in agreement with previous experiments performed on FTU, which highlighted that both the line-averaged density corresponding to the onset of a 2/1 TM and to the density limit are functions of the toroidal magnetic field only [8], with best fit values given by $\bar{n}_{MHD} = 0.19 \times B_T^{1.3}$ and $\bar{n}_{DL} = 0.19 \times B_T^{1.5}$, respectively. The critical mode amplitudes obtained in the analyzed pulses are reported in figure 3, where it is possible to see that the threshold for the onset of the limit

cycles decreases for increasing toroidal magnetic fields (left side) and increases for increasing plasma currents (center), showing essentially a dependence on the safety factor at the edge (right side). In particular, the only (B_T, I_p) configuration in figure 3 without marked limit cycles with increasing area is that one with $B_T = 4$ T and $I_p = 0.9$ MA, characterized by a value of the safety factor at the edge $q_a < 3$. This result has been confirmed in many pulses, also in others configurations obtained changing slightly the plasma current, always keeping $q_a < 3$, so our experiments seem to indicate that the presence of the $q = 3$ resonance in the plasma is necessary for the occurrence of deep and regular limit cycles for the 2/1 TM. It is worth noting that many plasma features change with the edge safety factor (e.g. the current density profile), so other experiments are required for a better comprehension of such an interesting phenomenon.

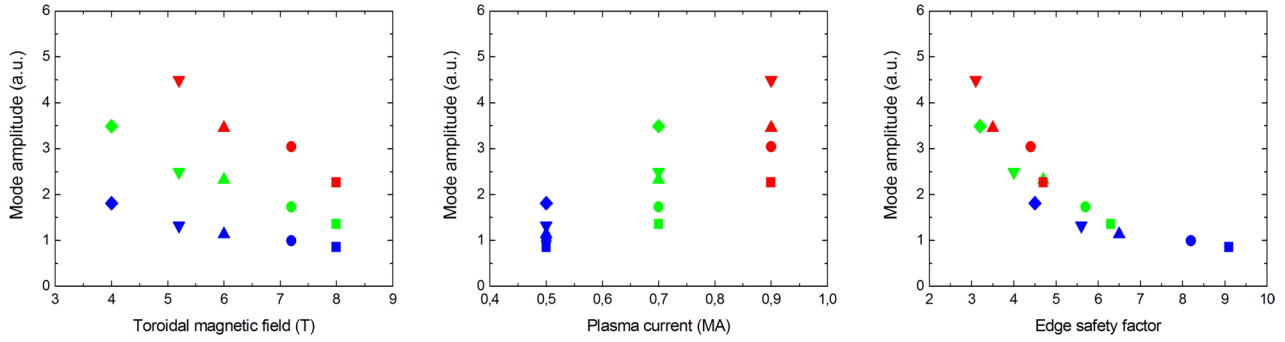


Figure 3. Critical mode amplitude for transition from smooth to cyclic behavior, as a function of the toroidal magnetic field (left side), plasma current (center) and safety factor at the edge (right side). Different symbols are used for different B_T and different colors are used for different I_p .

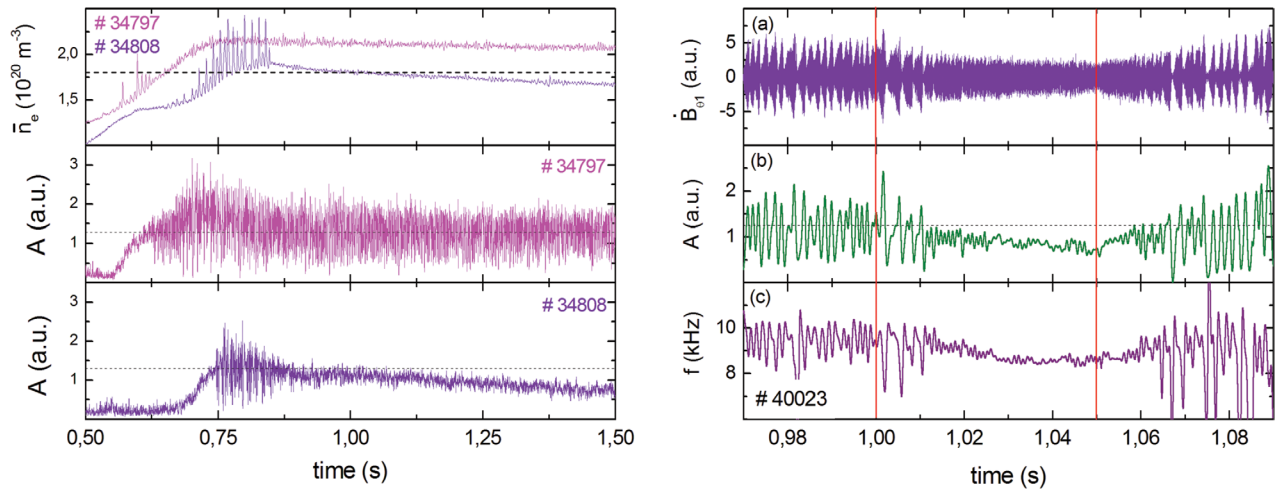


Figure 4. (Left side) Line-averaged density and mode amplitude for two pulses with $B_T = 5.2$ T and $I_p = 0.5$ MA. The spikes observed on the density signals (top panel) are associated to the MARFE instability and they are not correlated to the limit cycles. (Right side) Example of partial suppression of the 2/1 TM in FTU pulses at high density, by using injection of ECW: (a) output from the pick-up coil, (b) mode amplitude, (c) mode frequency. Red vertical bars indicate the ECW stage.

A more accurate experiment evidencing the existence of a well defined critical mode amplitude for transition from smooth to cyclic behavior has been performed, always changing the line-averaged density during the pulse. The result of such experiment is reported in figure 4 (left side). A first pulse (#34797), with $B_T = 5.2$ T and $I_p = 0.5$ MA, is realized with a flat-top density of about $2.1 \times 10^{20} \text{ m}^{-3}$, showing a transition to the bursting stage at a density of $1.8 \times 10^{20} \text{ m}^{-3}$, corresponding to a mode amplitude of 1.3 (in a.u.), and the presence of permanent limit cycles in the flat-top density stage. Then a second pulse (#34808), with same values for B_T and I_p , has been realized with a density increasing up to $1.9 \times 10^{20} \text{ m}^{-3}$ and afterward descending to $1.7 \times 10^{20} \text{ m}^{-3}$, and in this case it is possible to see a first transition from regular to bursting stage and a second transition from bursting to regular stage, in correspondence to the previously found critical mode amplitude. The existence of a well defined critical mode amplitude for transition from smooth to cyclic behavior has been also confirmed in experiments of real time control of TM performed on FTU by using injection of electron cyclotron waves (ECW) inside the 2/1 magnetic island [11]. In pulses of this kind, a partial suppression of the 2/1 TM is obtained during the ECW stage and a transition from cyclic

to smooth behavior is correspondingly observed (see figure 4, right side). On the other hand, when the ECW injection is stopped, the mode amplitude newly increases and a transition from smooth to cyclic behavior is observed.

5. Limit cycles on the phase-space

For a more detailed analysis of the MHD limit cycles, the time traces of some relevant quantities for a given cycle of the MHD activity illustrated in figure 1 are reported in figure 5 (left side), while in figure 5 (right side) the temporal evolution of the MHD mode for the same cycle is reported on the amplitude/frequency plane. The first important observation is that, whilst the evolution of the mode amplitude and frequency envelopes (see figure 2, right side) occurs in characteristic times (depending on the slope of the density ramp-up) of the order of the diffusion resistive time of about two hundred milliseconds (computed considering as length scale the radius of the $q = 2$ resonance), the mode amplitude increase and the subsequent decrease during a single limit cycle occur in a total time of 3.5 ms (see figure 5, left side), which is strongly lower than the diffusion resistive time. The second important

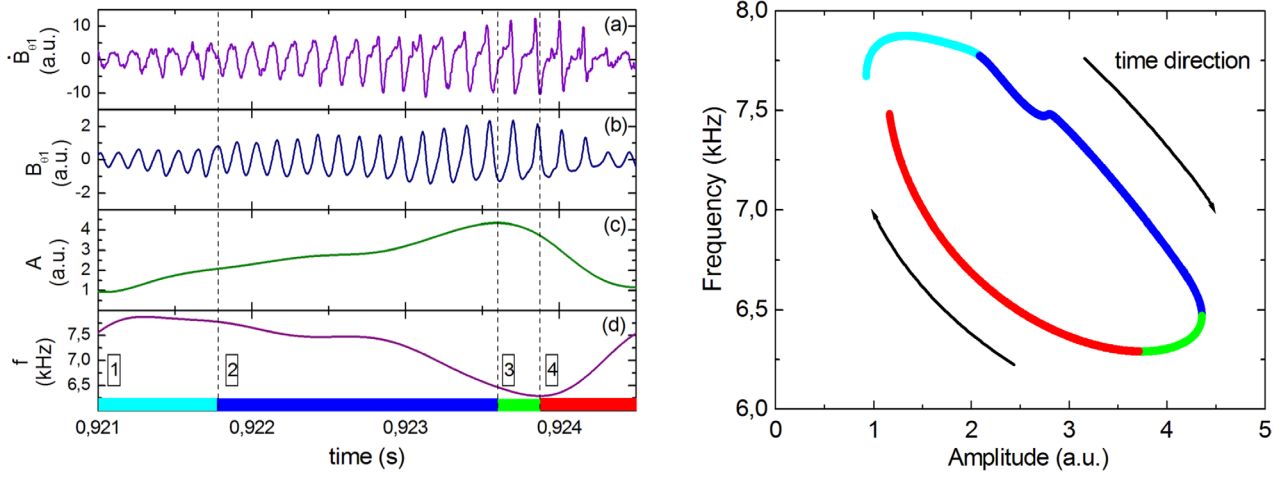


Figure 5. (Left side) Time traces of some relevant quantities for a given cycle of the MHD activity: (a) output from the pick-up coil, (b) poloidal magnetic perturbation, (c) mode amplitude, (d) mode frequency. (Right side) Temporal evolution (clockwise) of the MHD activity on the amplitude/frequency plane. Pulse #34843.

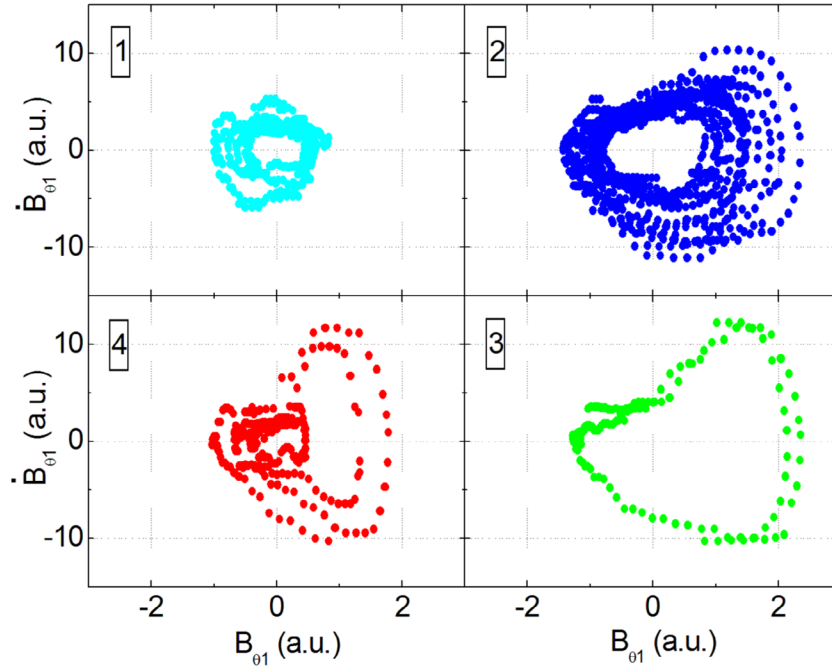


Figure 6. Diagrams in the phase-space $(B_{\theta 1}, \dot{B}_{\theta 1})$ for the oscillations in the four different stages of a limit cycle. Pulse #34843.

observation is that for a given limit cycle it is possible to distinguish four stages (see figure 5): a first stage (cyan) with increasing amplitude and approximately constant frequency, a second stage (blue) with increasing amplitude and decreasing frequency, a third stage (green) with decreasing amplitude and decreasing frequency, and a fourth stage (red) with decreasing amplitude and increasing frequency.

For the purpose of this work, we can try to understand the closed trajectories on the amplitude/frequency plane by considering the diagrams produced on the phase-space $(B_{\theta 1}, \dot{B}_{\theta 1})$ from the 25 oscillations due to the rotation of the magnetic island into the tokamak in the four different stages of the limit cycle considered in figure 5 and comparing these diagrams with those produced by a harmonic oscillator (see figure 6). As we can see, only on the first stage, characterized by an

increasing amplitude and a constant frequency, the behavior of the magnetic island rotation is like a harmonic oscillator, whilst in the third stage, characterized by decreasing amplitude and decreasing frequency, we have a very complex behavior, greatly different with respect to a harmonic oscillator. In order to highlight the importance of non-linear effects as a possible explanation for the different diagrams in figure 6, two different oscillations of the poloidal magnetic perturbation associated to the magnetic island, corresponding to the first and the third stage in figure 6, are reported in figure 7 (the two signals have been normalized in time). As we can see, the fundamental component is sufficient to fit the oscillation in the first stage (figure 7, left side), whilst the second and the third harmonic contributions are necessary in the third stage (figure 7, right side). On the other hands, the signals

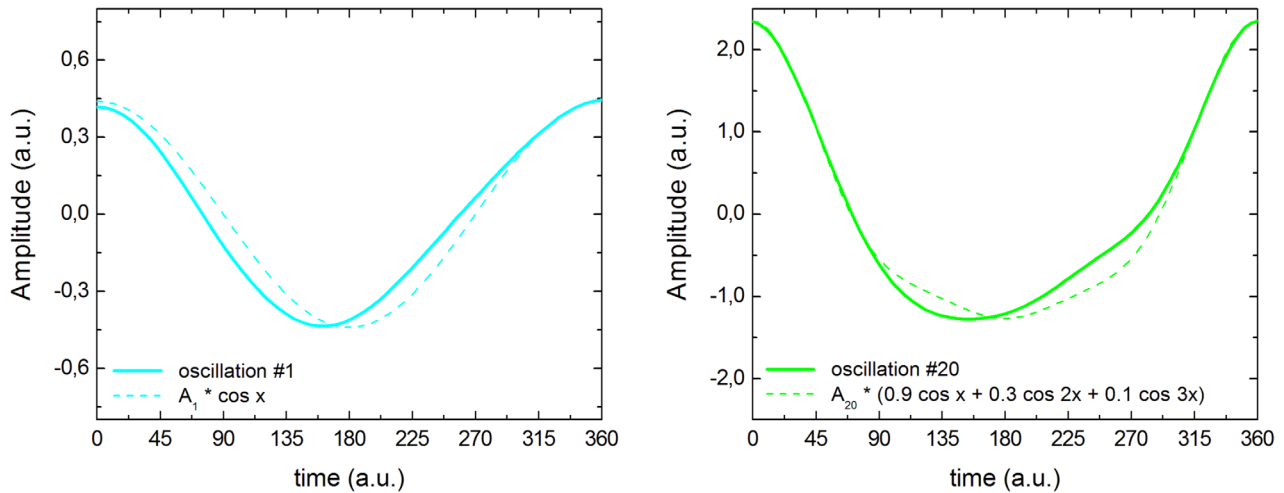


Figure 7. Oscillations of the poloidal magnetic perturbation (solid lines) in the first (left side) and the third (right side) stage of the limit cycle reported in figure 6. The contributions of the different harmonics are specified in the panels and the final fits are reported as dashed lines. Pulse #34843.

reported in figure 7 are representative snapshots of the island structure corresponding to the two different stages of the limit cycle, so that this result can be seen as an indication of a clear distortion increasing before amplitude drop (in particular, the distortion at the resonant surface is still higher in presence of harmonics), as evidenced by the importance of overtones, supporting the hypothesis of a recursive island fragmentation mechanism. The possibility of island fragmentation is suggested by the observation of secondary O-points in numerical simulations of islands formed by static error fields and stressed by plasma rotation [12]. It is necessary to highlight that this suggestive hypothesis is only a speculation, and dedicated studies are required to understand this phenomenon.

6. Conclusions

The MHD activity approaching the density limit shows an $m/n = 2/1$ tearing mode growing up to high amplitude, with a final stage characterized by amplitude and frequency oscillations, giving rise to limit cycles on the amplitude/frequency plane. In the cyclic stage the amplitude modulation is up to 80%, whilst the frequency modulation is up to 15%. The existence of a well defined critical mode amplitude for transition from smooth to cyclic behavior has been evidenced in experiments performed changing the line-averaged density, and in experiments of real time control of tearing mode by means of electron cyclotron resonance heating. These limit cycles could be due either by a recursive island fragmentation mechanism, or

by interaction with modes of different helicity. The performed experiments seem to indicate that the presence of the $q = 3$ resonance in the plasma is necessary for the occurrence of deep and regular limit cycles for the $2/1$ tearing mode and suggest that the island distortion increases before amplitude drops. A more accurate analysis will be done to confirm our preliminary results and to better understand the physical mechanisms responsible for this particular phenomenon observed for the $2/1$ tearing mode in the high density regime on FTU.

References

- [1] Lawson J.D. 1957 *Proc. Phys. Soc. B* **70** 6
- [2] Greenwald M. 2002 *Plasma Phys. Control. Fusion* **44** R27
- [3] Furth H.P., Rutherford P.H. and Selberg H. 1973 *Phys. Fluids* **16** 1054
- [4] Waddell B.V. et al 1978 *Phys. Rev. Lett.* **41** 1386
- [5] Sykes A. and Wesson J.A. 1980 *Phys. Rev. Lett.* **44** 1215
- [6] Nave M.F.F. and Wesson J.A. 1990 *Nucl. Fusion* **30** 2575
- [7] Gormezano C. et al 2004 *Fusion Sci. Technol.* **45** 297
- [8] Pucella G. et al 2013 *Nucl. Fusion* **53** 083002
- [9] Pucella G. et al 2013 *Proc. 40th EPS Conf. on Plasma Physics (Espoo, Finland, 1–5 July 2013)* vol 37D (ECA) P5.139 (<http://ocs.ciemat.es/EPS2013PAP/pdf/P5.139.pdf>)
- [10] Pucella G. et al 2015 *Proc. 42nd EPS Conf. on Plasma Physics (Lisbon, Portugal, 22–26 June 2015)* vol 39E (ECA) P4.112 (<http://ocs.ciemat.es/EPS2015PAP/pdf/P4.112.pdf>)
- [11] Sozzi C. et al 2015 *Nucl. Fusion* **55** 083010
- [12] Ishii Y., Azumi M. and Smolyakov A.I. 2007 *Nucl. Fusion* **47** 1024